


Massive Stars in Low-metallicity Galaxies in the CLASSY Survey

Danielle A. Berg¹ , Beth L. James², Teagan King³,
Meaghan McDonald³, Zuyi Chen⁴, John Chisholm¹,
Timothy Heckman⁵, Crystal L. Martin⁶, Dan P. Stark⁴
and The CLASSY Team⁷

¹Department of Astronomy, The University of Texas at Austin,
2515 Speedway, Stop C1400, Austin, TX 78712, USA
email: daberg@austin.utexas.edu

²AURA for ESA, Space Telescope Science Institute,
3700 San Martin Drive, Baltimore, MD 21218, USA

³Space Telescope Science Institute,
3700 San Martin Drive, Baltimore, MD 21218, USA

⁴Steward Observatory, The University of Arizona,
933 N Cherry Ave, Tucson, AZ, 85721, USA

⁵Center for Astrophysical Sciences, Department of Physics & Astronomy,
Johns Hopkins University, Baltimore, MD 21218, USA

⁶Department of Physics, University of California,
Santa Barbara, Santa Barbara, CA 93106, USA

⁷39 collaborators worldwide

Abstract. Rest-frame far-ultraviolet spectra are fundamental to our understanding of star-forming galaxies, providing a unique window on massive star populations (MSs), chemical evolution, feedback processes, and reionization. JWST is ushering in a new era, pushing the FUV frontier beyond $z=10$. The success of such endeavors hinges on a comprehensive understanding of the MSs and gas conditions that power the observed spectra. The COS Legacy Archive Spectroscopic SurveY (CLASSY) is a powerful and promising solution providing high-quality, high-resolution FUV spectra of 45 nearby star-forming galaxies. The spectra contain a suite of features that simultaneously characterize the MSs that populate metal-poor galaxies, physical properties of large-scale outflows, and chemical abundance patterns. The CLASSY sample is consistent with the $z=0$ mass-metallicity relationship and spans 1.5 dex in metallicity. These unique properties make CLASSY the benchmark training set for studies of MSs in star-forming galaxies both across cosmic time and connecting metal-poor to metal-rich populations.

Keywords. atlases, galaxies: star clusters, stars: winds, outflows, stars: mass loss

1. Introduction

Massive stars are fundamental to our understanding of the baryon cycle and galaxy evolution in general. The size of the gas reservoir from which stars form is regulated by the balance between gas accretion from the cosmic web, the rate at which stars form from this gas, and gas loss from galaxies. Gas may be driven out of galaxies by feedback, including stellar winds, super novae explosions, and the energetic radiation from hot gas falling into super massive black holes found at the center of galaxies, called active galactic nuclei

feedback. Additionally, the ionizing spectra of massive stars are not yet well-understood. The extreme-UV (EUV) radiation field they produce is reprocessed by the interstellar medium (ISM), powering the observed nebular emission lines. Uncertainties in the form of the ionizing spectrum thus have a significant effect on the interpretation of the nebular lines. While the implementation of new physics in stellar population synthesis (SPS) models (i.e., rotation, binaries) continues to improve predictions of the EUV radiation field (e.g., [Levesque et al. 2012](#); [Eldridge et al. 2017](#); [Götberg et al. 2018](#)), the shape of the ionizing spectrum remains very poorly constrained for the metal poor ($Z/Z_{\odot} < 0.2$) stellar populations that come to dominate at high redshift. Therefore, to truly understand cosmic galaxy evolution, we must study both the stars and the gas within the same systems.

1.1. *The Diagnostic Power of the FUV*

The far-ultraviolet (FUV), defined here as $\sim 1200 - 2000 \text{ \AA}$, is arguably the richest wavelength regime in diagnostic spectral features characterizing stellar and nebular processes and will provide an important window onto the first generation of galaxies in the forthcoming era of extremely large telescopes (ELTs) and the James Webb Space Telescope (JWST). In particular, several spectral features characterize the (1) hot, massive stars that dominate feedback processes and are observed as prominent wind features ($1240 < \lambda < 1720$) produced in the expanding atmospheres of O- and B-stars and are brightest in the FUV (e.g., [Leitherer et al. 1999](#)); (2) resonant interstellar absorption lines (see [Veilleux et al. 2005](#)) and associated non-resonant (“fine-structure”) emission lines (e.g., [Shapley et al. 2003](#)) that trace both the static ISM and galactic outflows ($1240 < \lambda < 1854$); (3) emission lines ($1390 < \lambda < 1910$; e.g., [Kinney et al. 1993](#)) that are produced by collisional excitation or recombination in gas that is photoionized by the hot, massive stars (e.g., [Schaerer 2003](#)); and (4) Ly α profiles ($\lambda = 1215 \text{ \AA}$), which is typically nebular in origin, entrains details of the outflowing gas and predicts the escape of ionizing radiation (e.g., [Wofford et al. 2013](#); [Rivera-Thorsen et al. 2015](#); [Verhamme et al. 2015](#); [Gronke 2017](#)). All of these features are shaped, in some way, by the radiation, energy, and/or momentum produced by massive stars. The range and richness of features in the FUV is demonstrated in Figure 1.

2. The CLASSY Survey

The new release of the COS Legacy Archive Spectroscopic Survey (CLASSY; [Berg et al. 2022](#)) offers a powerful and promising opportunity to study massive star populations. The CLASSY atlas is the first high-quality, high-resolution FUV spectral catalog of star-forming galaxies at $z \sim 0$, enabling detections of the nebular lines together with faint stellar absorption lines. To optimize the scientific utility of the CLASSY FUV spectral atlas, it provides: (1) Broad wavelength coverage to simultaneously probe the continuum, absorption, and emission features that characterize the stellar populations and gas of the galaxy. (2) High spectral resolution. Theory predicts that the velocities of galactic outflows scale with the circular velocities of their host galaxies (e.g., [Murray et al. 2005](#)). Therefore, CLASSY has very high spectral resolution ($R > 10,000$ or velocity resolution less than 30 km s^{-1}) allowing measurements of the impact of stellar feedback in galaxies, event at low stellar-mass (see, e.g., [McGaugh 2001](#)). (3) High signal-to-noise (S/N) in the continuum, allowing faint stellar features to be significantly detected and measured.

2.1. *Sample Properties*

CLASSY combines 135 orbits of new Hubble Space Telescope (HST) / Cosmic Origins Spectrograph (COS) data with 177 orbits of archival HST data, for a total of 312

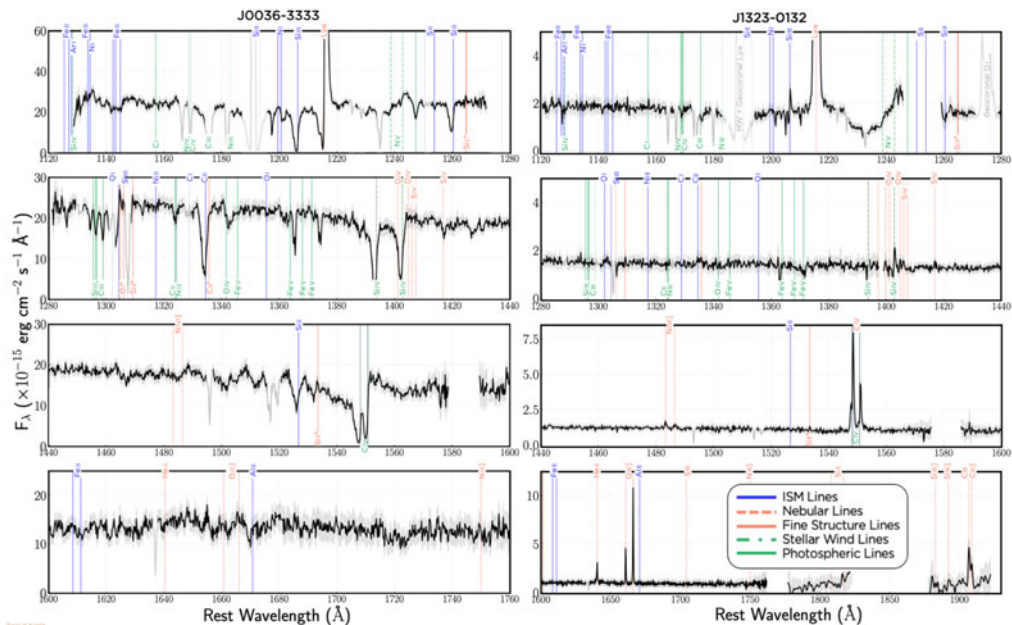


Figure 1. CLASSY spectra demonstrating the numerous diagnostic features present in the FUV. *Left:* The spectrum of the metal-rich galaxy J0036-3333 is rich with stellar wind features (dot-dashed green lines), such as the SiIV and CIV features, and interstellar medium absorption lines (solid blue lines), including the strong SiII and CII features. J0036-3333, however, contains no significant UV emission features besides Ly α λ 1215. *Right:* The spectrum of the metal-poor galaxy J1323-0132 is strikingly different than that of J0036-3333. In particular, the spectrum has strong emission features from Ly α , CIV, HeII, OIII], and CIII] and additional weak detections from the high-ionization OIV, SiV, and NiV] lines, but minimal absorption features. Figures adopted from Berg *et al.* (2022).

orbits, to complete an atlas of 45 local star-forming galaxies. In order to achieve nearly-panchromatic FUV spectral coverage with the highest spectral resolution possible, CLASSY efficiently augments existing archival data with new HST/COS observations, uniting the high-resolution G130M, G160M, and G185M gratings for a sample of galaxies spanning broad parameter space. As a result, CLASSY provides a well-controlled local FUV sample with the requisite sensitivity and spectral resolution to enable synergistic studies of stars and gas within the *same* galaxies. The CLASSY sample properties are shown in Figure 2.

3. High Level Science Products

CLASSY is a treasury program that is providing a number of state-of-the-art data products to the astronomical community in digital form to ensure their enduring value and utility. The primary data products are the high-resolution, high-S/N coadded multi-grating FUV spectral templates of the CLASSY sample of 45 star-forming galaxies. Additional planned data products include stellar continuum fits, nebular abundance measurements, improved UV emission line diagnostics, feedback properties, radiative transfer models, and more. With these high-level science products (HLSPs), the CLASSY Treasury will complete the vital picture that is needed to diagnose the suite of star-forming galaxy properties that will be offered to us in the next decade. Given the uncertain future of observed-frame UV capabilities, the CLASSY templates and models embody an indispensable toolset.

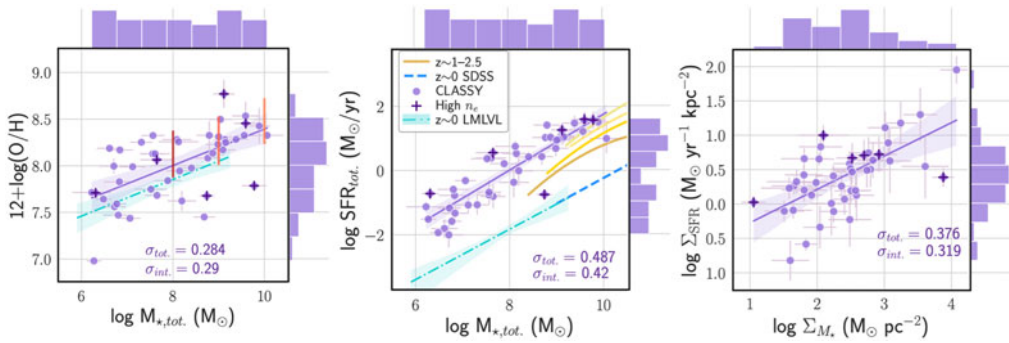


Figure 2. CLASSY sample properties, as measured from optical spectra and UV+optical photometry (see Berg et al. 2022), span a broad range of parameter space. *Left:* Gas-phase oxygen abundance is plotted relative to total stellar mass, showing the well-known mass-metallicity relationship. The CLASSY sample seems to follow the same trend as other normal star-forming galaxies (e.g., Berg et al. 2012; Curti et al. 2020), but with larger scatter. *Middle:* Star formation rate is plotted versus stellar mass for both the entire galaxy and in terms of surface density (*right*). The middle plot shows a trend that extends to lower masses and star formation rates, but lies above the previous galaxy sample studies at $z \sim 0$ (SDSS: Chang et al. (2015); blue dashed line and LMLVL: Berg et al. (2012) and Lee et al. (2009); cyan dot-dashed lines) and $z \sim 1 - 2.5$ (Whitaker et al. 2014, yellow lines). Figure adapted from Berg et al. (2022).

The first HLSP, the CLASSY FUV spectral atlas of star-forming galaxies, has been released on two main platforms. First, all CLASSY HLSPs will be available via the CLASSY HLSP home page: <https://archive.stsci.edu/hlsp/classy>, which also serves as the main website for the CLASSY Treasury and relevant information. Importantly, this website provides simple tarball downloads of individual CLASSY HLSPs, as well as the entire CLASSY HLSP data collection. In addition to full data access, the CLASSY HLSP home page provides machine-readable table downloads for the tables of properties in the CLASSY I paper (Berg et al. 2022), interactive spectra that allow quick-look examination of the coadded spectral features, user-friendly jupyter notebook guides to accessing and using the CLASSY HLSPs, and important links such as to the NASA Astrophysics Database System (ADS) library of CLASSY publications.

The second platform for accessing the CLASSY HLSPs is the Mikulski Archive for Space Telescopes (MAST) via the CLASSY MAST website: <https://mast.stsci.edu/search/ui/#/classy>. The MAST portal provides a unique search-and-selection method to access the HLSPs, where users can select a subsample of the data products based on HLSP type, filename, or target properties such as coordinates or stellar mass. This search tool will continue to be developed based on the specifics of each HLSP release in order to allow more efficient and straightforward access to data products that are of interest to the user. In this manner, appropriate subsets of the CLASSY HLSPs can easily be selected for a given scientific analysis, to match specific survey sample properties, and more.

3.1. HLSP 1: The CLASSY Spectral Atlas

The primary HLSPs of the CLASSY treasury survey are high S/N multi-grating coadded spectra. The coadded spectra were carefully constructed from multi-grating HST/COS datasets with different spectral resolution and varying degrees of vignetting and degradation in spectral resolution depending on the shape of their overall UV light profile entering the COS aperture. The complicated CLASSY dataset can also be used as a strength to produce four spectral coadds for each galaxy with different resolutions: (1) The Very High Resolution (VHR) Coadds: consisting of only G130M spectra, which have

a nominal point source resolution of $9.97 \text{ m}\text{\AA}/\text{pixel}$ or $0.060 \text{ \AA}/\text{resel}$. This is the highest spectral resolution of the CLASSY gratings. (2) The High Resolution (HR) Coadds: consisting of the CLASSY medium-resolution FUV gratings, or G130M+G160M spectra, with a nominal point source resolution of $12.23 \text{ m}\text{\AA}/\text{pixel}$ or $0.073 \text{ \AA}/\text{resel}$. (3) The Moderate Resolution (MR) Coadds: consisting of the CLASSY FUV+NUV medium resolution gratings, or G130M+G160M+G185M+G225M spectra, with a nominal point source resolution of $33 \text{ m}\text{\AA}/\text{pixel}$ or $0.200 \text{ \AA}/\text{resel}$. (4) The Low Resolution (LR) Coadds: consisting of the CLASSY medium and low resolution gratings. Possible grating combinations include G130M+G160M+G140L and G130M+G160M+G185M+G225M+G140L, with a nominal point source resolution of $80.3 \text{ m}\text{\AA}/\text{pixel}$ or $0.498 \text{ \AA}/\text{resel}$.

Examples of high-quality moderate-resolution CLASSY coadded spectra is shown in Figure 1. The different spectral dispersion of the coadds allow CLASSY to be used for many scientific studies that require a range of spectral resolutions. These coadds provide both high resolution spectra over the $\sim 1200 - 1700 \text{ \AA}$ range of each object that is important to studies of stellar and ISM absorption features and contiguous FUV $\sim 1200 - 2000 \text{ \AA}$ wavelength coverage at low resolution that is necessary to simultaneously interpret the stars and gas.

Interestingly, few CLASSY galaxies are in previous FUV spectral atlases, making it difficult to directly compare them. Fortunately, International Ultraviolet Explorer (IUE) and CLASSY observations both exist for two galaxies: J0337-0502 (SBS 0335-052 E) and J0934+5514 (I Zw 18 NW). For a visual comparison, the HST and IUE spectra for J0337-0502 are plotted in Figure 3, showing substantial, but expected differences. The smaller aperture of COS ($2.5''$) relative to the IUE ($10'' \times 20''$ aperture) records lower UV continuum fluxes (however, this would not be expected for most of the NUV-compact CLASSY sample) and some features are present in only the IUE spectrum, which also contains the W cluster region. For example, there appear to be weak emission features present just blueward of 1400 \AA and at 1750 \AA , likely NIII], that are emitted by the E region but not the W region. Perhaps the most important difference, though, is the significant number of features and details revealed by the higher resolution of the CLASSY spectra ($\sim 0.1 \text{ \AA}$ resolution compared to the $\sim 6 \text{ \AA}$ of the IUE spectrum). Specifically, a number of significant ISM absorption lines and nebular emission lines are recovered, such as the OI and SiII lines shown in the left-most inset window of Figure 3 and the CIV, HeII, OIII], and CIII] lines shown in the other three inset windows.

Figure 3 clearly demonstrates that the CLASSY survey provides a dramatic leap forward in FUV spectral atlases and is an invaluable tool for the interpretation and modeling of star-forming galaxies across redshifts. The variety of CLASSY galaxies also results in a diversity of spectra. More metal-poor, low-mass galaxies are generally rich with nebular emission lines, but lacking in strong ISM absorption lines or stellar features. On the other hand, more metal-rich, massive galaxies tend to have weak to no emission lines, but many ISM absorption lines and stellar features.

3.2. HLSP 2: The CLASSY Stellar Continuum Fits

The UV stellar continuum is a powerful tool to characterize the ionizing stellar population, sensitive to the most recent $\sim 40 \text{ Myr}$ of star formation. It is also important to resolve the contribution of the stellar, ISM, and narrow nebular (intrinsic widths typically 10s of km s^{-1}) features to disentangle their contributions to the emission line profile. SPS model fits to the stellar continuum are largely constrained by two different stellar features (see Figure 1): (1) the broad wind features from young O-stars and (2) the weak photospheric absorption lines from both O- and B-stars. Even at low-metallicities, these two types of stellar continuum features constrain the stellar population age. The

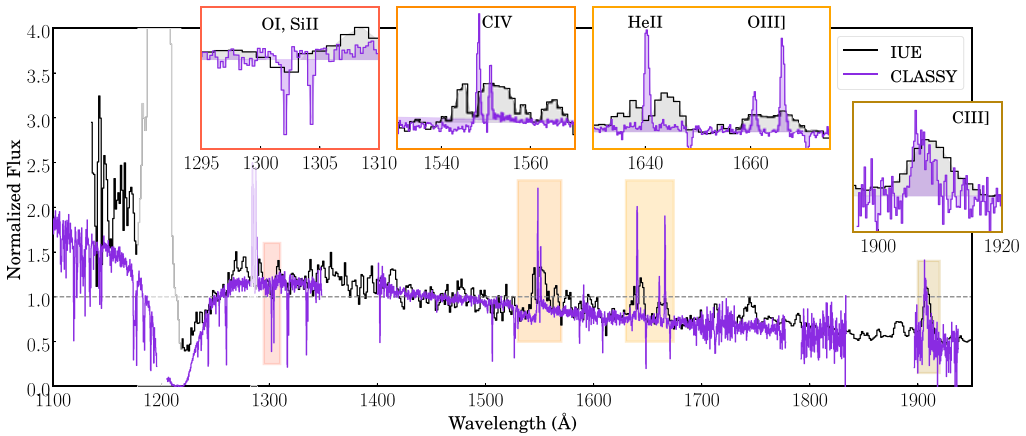


Figure 3. Comparison of rest-frame spectra for J0337-0502 (SBS 0335-052) to demonstrate the improvement of the CLASSY survey over previous FUV spectral atlases. The IUE spectrum is relatively low resolution ($\lambda/\Delta\lambda \sim 300$) and consists of the integrated light within its large $10'' \times 20''$ aperture. In contrast, the CLASSY coadded spectral templates are characterized by an unrivaled combination of contiguous 1200–2000 Å FUV wavelength coverage, high spectral resolution ($\lambda/\Delta\lambda \sim 15,000$), and high S/N (average S/N = 6.4 per resel). Additionally, the $2.5''$ COS aperture better targets compact regions such as massive star clusters. Both spectra are normalized at 1450 Å. Note that the breaks in the CLASSY spectrum are due to chip gaps and that the Geocoronal Ly α and OI emission have been whited-out. While few features are apparent in the IUE J0337-0502 spectra, the CLASSY spectrum reveals a significant number of absorption and emission features that enable simultaneous studies of the massive stellar population, ISM outflows, and nebular emission. Figure adopted from Berg et al. (2022).

spectra of young stars are dominated by the prominent P-Cygni features from the stellar winds which have deep and broad absorption extending to over $\sim 5000 \text{ km s}^{-1}$ from line center and broad emission redward of line center. P-Cygni features indicate that the stellar population is less than 5 Myr old and the P-Cygni features rapidly decrease at older ages. This is because stars older than 5 Myr do not drive significant stellar winds. These features provide robust age estimates of the young stellar population. The weak blue absorption portion of the P-Cygni features is sufficiently offset in velocity-space from the observed nebular emission (with observed emission only to $\sim 1500 \text{ km s}^{-1}$), but the red P-Cygni emission will be blended with the strong high-ionization emission lines. It is, therefore, crucial to our science objectives to accurately model the P-Cygni profile and remove it from the nebular emission. Consequently, the narrow photospheric features provide a critical secondary feature to determine the age, and, in turn, the predicted continuum shape near the high-ionization lines.

CLASSY stellar continuum fits will soon be available on the CLASSY HLSP website and will be presented in Senchyna et al. (2022). The observed CLASSY stellar continua were fit using a linear combination of the single-aged fully-theoretical stellar continuum models. The fitting method follows the fully-tested fitting procedure of Chisholm et al. (2019), which accurately reproduces the shapes of high-ionization stellar features in local and high-redshift galaxies (e.g., Chisholm et al. 2016; Rigby et al. 2018). The CLASSY fits explore a suite of available stellar libraries, that include single and binary stars (i.e., STARBURST99, BPASS; Leitherer et al. 2010; Conroy & Gunn 2010; Stanway et al. 2016), updated models of Wolf-Rayet stars (the new Bruzual & Charlot models), and the full array of available stellar metallicities.

The resulting stellar population fits estimate mean stellar ages and continuum metallicities. Removing the fitted stellar continua isolates the true nebular emission, allowing

FUV emission lines to be used for nebular diagnostics diagnostic diagram. Additionally, the stellar continuum fits can be used as inputs to cloudy photoionization models to test the production of the observed emission lines.

4. Pilot Study of Two Metal-Poor Extreme Emission Line Galaxies

Bright high-ionization nebular emission-lines present our best tool to detect and characterize the most distant star-forming galaxies that JWST will observe, yet the physics governing their production is poorly understood. Galaxies containing prominent detections of these high-ionization CIV $\lambda\lambda 1548,50$, HeII $\lambda 1640$, OIII] $\lambda\lambda 1661,66$, and CIII] $\lambda\lambda 1907,09$ are referred to as extreme emission line galaxies (EELGs). Such high-ionization emission requires especially hard ionizing-radiation, where current models of massive stars predict few photons. A number of alternative mechanisms have been proposed to produce the hard ionizing radiation in EELGs, including very massive metal poor stars, stripped stars (e.g., [Götberg et al. 2017, 2019, 2020](#)), ultra luminous X-ray sources (e.g., [Schaerer et al. 2019](#)), high-mass X-ray binaries (e.g., [Eldridge et al. 2017](#)), and accreting IMBHs ([Thuan & Izotov 2005](#)).

Here we investigate the massive star populations of two EELGs in CLASSY, J1044+0353 and J1418+2102, and how their ionizing spectra impact the observed FUV spectra. Recently, we fit the observed stellar continuum using a linear combination of single-aged fully-theoretical models in [Olivier et al. \(2022\)](#). The resulting fit, shown for J1044+0353 in Fig. 4, characterizes the ionizing spectral energy distribution (SED) of the current burst of star formation ($\lesssim 40$ Myr), providing the luminosity-weighted age, metallicity, and reddening of the stellar population. Subtracting the stellar continuum fit reveals high-ionization UV emission lines that are well-fit by narrow, nebular Gaussian profiles. These lines (i.e., SiIV $\lambda\lambda 1393,1403$, OIV $\lambda\lambda 1401,05,07$, SiV $\lambda\lambda 1405,06,17$, CIV $\lambda\lambda 1548,50$, HeII $\lambda 1640$, and OIII] $\lambda\lambda 1661,66$) can be used as nebular diagnostics.

To test whether massive stars have drive the observed emission line fluxes, we ran a suite of cloudy photoionization models with the best-fit stellar models as the input ionizing source and the measured nebular properties as Gaussian priors. Comparing the resulting emission line fluxes produced by the massive star population to the observed nebular emission lines reveals that the stellar models are able to produce the entire suite of moderate- to low-ionization ($\lesssim 35$ eV) emission lines, but failed to reproduce higher ionization lines. The difference between the predicted and observed high- and very-high ionization lines then provide tight constraints of the strength and shape of high-energy flux from non-stellar sources needed to match the observations.

[Olivier et al. \(2022\)](#) employed this method and demonstrated that employing a self-consistent model of the measured ionizing stellar population and full suite of emission lines spanning a wide range of energies does indeed highly constrain the full ionizing SED shape. They then added a blackbody to the stellar populations fit from the UV continuum to model the necessary high-energy photons to reproduce the very-high ionization lines (e.g., HeII, [OIV]). As shown in Figure 5, they found that a contribution from a blackbody of 80,000 K with $\sim 60 - 70\%$ of the luminosity from the young stellar population is needed to reproduce the entire suite of observed emission lines spanning low-, intermediate-, high-, and very-high ionization potentials.

This self-consistent modeling of the ionizing spectra of two nearby EELGs indicates the presence of a previously unaccounted-for source of hard ionizing photons, but what could this extra source of very-high-energy ionizing photons be? The low-metallicity nature of these sources calls into question the accuracy of the low-metallicity stellar atmosphere models. Further, observations of individual O stars below the 20% solar metallicity (Z_{\odot}) of the Small Magellanic Cloud (SMC) are incredibly rare and, thus, hamper our ability to model the ionizing fluxes of metal-poor stellar populations.

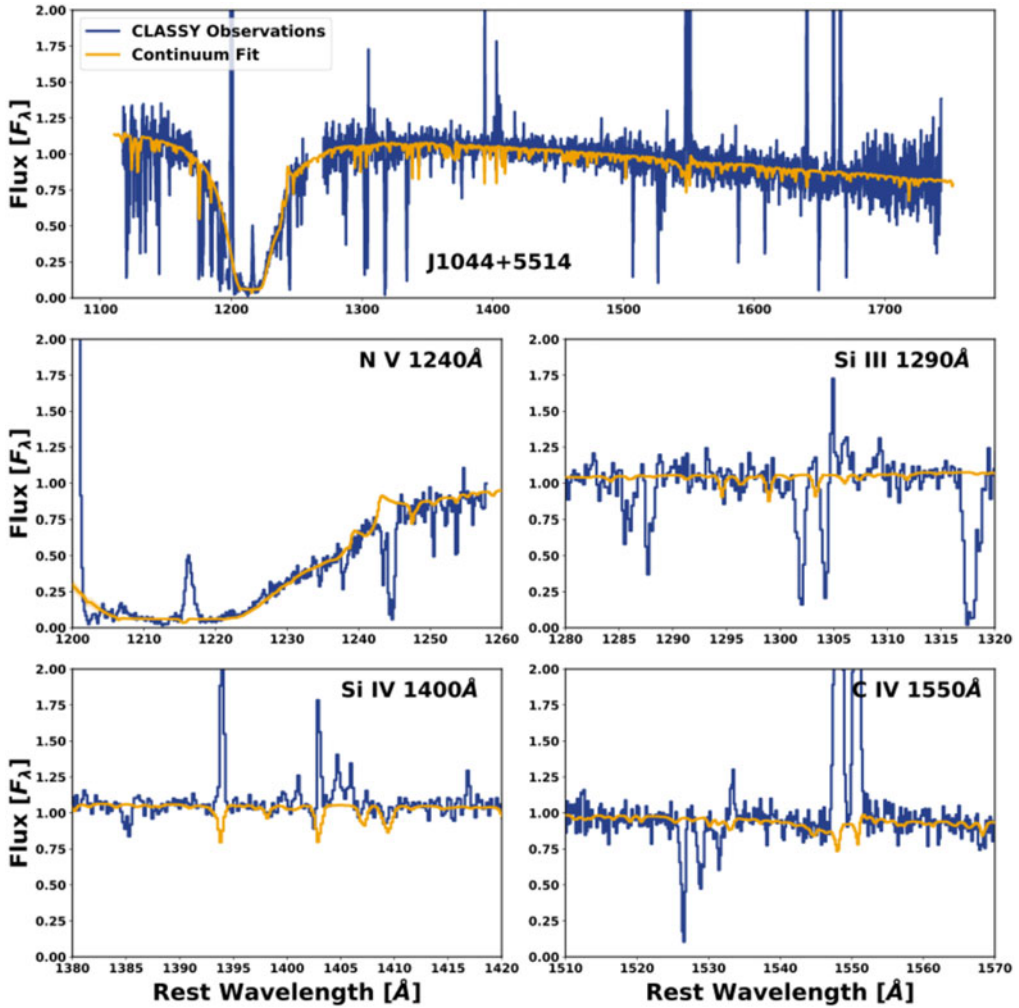


Figure 4. The CLASSY FUV spectrum of J1044+2102 and the best-fit massive star continuum model. The data are plotted in black and are normalized by their flux at 1495 Å. Over-plotted is the massive star population continuum fit from the STARBURST99 models (Leitherer et al. 1999) in gold.

To address this issue, Telford et al. (2021) presented the first-ever FUV spectra of three very metal-poor O-dwarf stars in the galaxies Leo P (3% Z_{\odot}), Sextans A (6% Z_{\odot}), and WLM (14% Z_{\odot}), shown in Fig. 6. Using this data, these authors demonstrated that the equivalent widths of photospheric metal lines and strengths of wind-sensitive features correlate with metallicity down to very low metallicities. They also used FUV through near-infrared SEDs to model the fundamental properties of the three stars. Comparing to FUV spectra of SMC stars with similar properties reveals two important insights about very metal poor stars: (1) the most metal-poor stars (represented by the star in Leo P) drive much weaker stellar winds than those seen at 20% Z_{\odot} from the SMC counterparts and (2) very metal-poor stars, as determined from the stars in Leo P and Sextans A, are fast-rotators with projects rotation speeds of $v \cdot \sin(i) \geq 290 \text{ km s}^{-1}$ (Fig. 6). Such high rotation speeds were unexpected: The probability of finding two fast rotators is just a 3%–6% if the metal-poor stars are drawn from the same $v \cdot \sin(i)$ distribution observed for O dwarfs in the SMC. These observations suggest that model improvements are needed

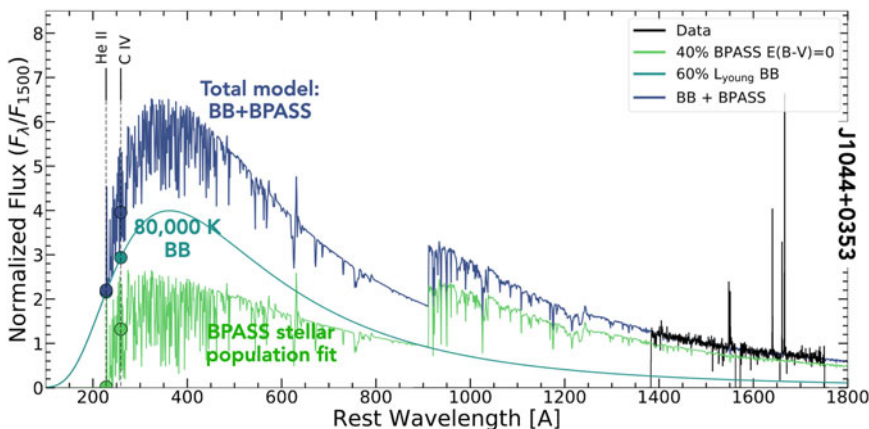


Figure 5. The ionizing X-ray+extreme-UV and non-ionizing FUV continua are shown for CLASSY galaxy J1044+0353 (labeled J1044). The overall self-consistent best-fit model is plotted as dark blue, and showing an excellent fit to both the observed massive star population continuum (black spectrum) and the very-high-ionization emission line strengths (dark blue circles). The best-fit model consists of (1) the binary-star (BPASS) massive star population continuum fit model to the observed FUV spectrum (lime green spectrum) plus (2) a blackbody with a luminosity of 60% of the total FUV luminosity (luminosity dominated by young stars) and a temperature of 80kK (teal spectrum). The teal circles show the intersection of each model with the wavelength required to produce He II and C IV, where both the blackbody and the stellar population models alone fail to reproduce the observed stellar+nebular spectrum.

to include the impact of rotation and weak winds on ionizing flux to accurately interpret observations of metal-poor galaxies in both the near and distant universe.

References

- Berg, D. A., Skillman, E. D., Marble, A., et al., 2012 *ApJ*, 754, 98
- Berg, D. A., Chisholm, J., James, B. L., Heckman, T., Martin, C. et al., 2022 accepted to *ApJ*
- Bouret, J. C., Lanz, T., Martins, F., et al., 2013 *A&A*, 555, A1
- Chang, Yu-Yen, van der Wel, Arjen, da Cunha, Elisabete, Rix, & Hans-Walter, 2015 *ApJ*, 219, 8
- Chisholm, J., Tremonti, C. A., Leitherer, C., Chen, Y., & Wofford, A., 2016 *MNRAS*, 457, 3133
- Chisholm, J., Rigby, J. R., Berg, D. A., Bayliss, M., Dahle, H., Gladders, M., & Sharon, K., 2019 *ApJ*, 882, 182
- Conroy, Charlie & Gunn, James E., 2010 *Astrophysics Source Code Library*, record ascl:1010.043
- Curti, M., Mannucci, F., Cresci, G., & Maiolino, R., 2020 *MNRAS*, 491, 944
- Eldridge, J. J., Stanway, E. R., Xiao, L., McClelland, L. A. S., et al., 2017 *PASA*, 34, 58
- Eldridge, J. J. & Stanway, E. R., 2022 *arXiv*, arXiv:2202.01413
- Götberg, Y., de Mink, S. E., & Groh, J. H., 2017 *A&A*, 615, 78
- Götberg, Y., de Mink, S. E., Groh, J. H., Kupfer, T., Crowther, P. A., Zapartas, E., & Renzo, M., 2018 *A&A*, 608, 11
- Götberg, Y., de Mink, S. E., Groh, J. H., Leitherer, C., & Norman, C., 2019 *A&A*, 634, 134
- Götberg, Y., de Mink, S. E., McQuinn, M., Zapartas, E., Groh, J. H., & Norman, C., 2022 *A&A*, 634, 134
- Gronke, Max, 2017 *A&A*, 608, 139
- Kinney, A. L., Bohlin, R. C., Calzetti, D., Panagia, N., & Wyse, R. F. G., 1993 *ApJS*, 86, 5
- Lee, J. C., Gil de Paz, A., Tremonti, C., Kennicutt, R. C., Jr., Salim, S., et al., 2009 *ApJS*, 706, 599
- Leitherer, C., Schaerer, D., Goldader, J. D., et al., 1999 *ApJS*, 123, 3
- Leitherer, C., Ortiz Otálvaro, P. A., Bresolin, F., et al., 2010 *ApJS*, 189, 309

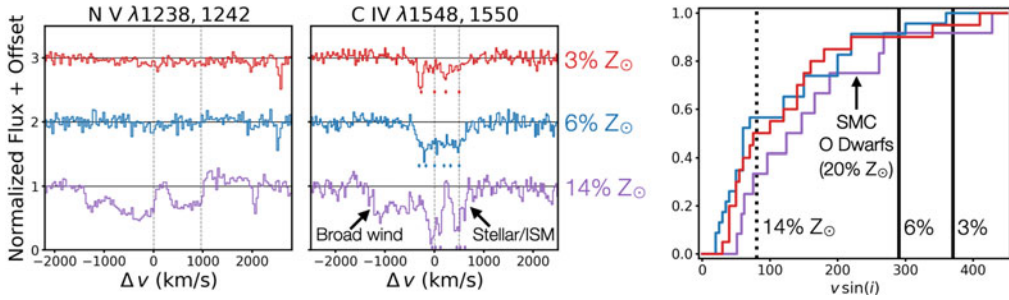


Figure 6. *Left:* Extremely low metallicity stars show weak stellar wind features, as demonstrated by the spectra of the LP26 star in Leo P (purple), the S3 star in Sextans A (blue), and the A15 star in WLM (red). The spectra are continuum-normalized, then offset, and plotted as a function Nv 1238 Å, Ov 1371 Å, Siv 1393 Å, and Civ 1548 Å. Diamonds below each spectrum indicate the velocities of ISM $SIII$ and CII absorption components detected. Broad, blueshifted CIV wind absorption is also present. A15 also shows wind absorption and emission in the Nv and Ov lines. All stars' Siv lines are likely due to photospheric and ISM absorption rather than winds. *Right:* The cumulative distribution of $v \cdot \sin(i)$ measured for O dwarfs in the SMC are plotted as colored lines, where each is from a different sample/study (Penny & Gies 2009; Bouret et al. 2013; Ramachandran et al. 2019). In comparison, the $v \cdot \sin(i)$ measured for the three metal-poor O dwarfs from Telford et al. (2021) are indicated with black vertical lines. Both LP26 and S3 have $v \cdot \sin(i)$ higher than 90% of the measurements for SMC O dwarfs. The two most metal poor stars, LP26 and S3, have $v \cdot \sin(i)$ higher than 90% of the measurements for SMC O dwarfs. Both figures adapted from Telford et al. (2021).

- Levesque, E. M., Leitherer, C., Ekstrom, S., Meynet, G., & Schaerer, D. 2012, *ApJ*, 751, 67
- McGaugh, S. S., Rubin, V. C., & de Blok, W. J. G., 2001 *AJ*, 122, 2381
- Murray, N., Quataert, E., & Thompson, T. A., 2005 *ApJ*, 618, 569
- Olivier, G.M., Berg, D. A., Chisholm, J., Erb, D.K., Pogge, R.W., & Skillman, E.D., 2022 accepted to *ApJ*
- Penny, L. R. & Gies, D. R., 2009 *ApJ*, 700, 844
- Ramachandran, V., Hamann, W. R., Oskinova, L. M., et al., 2019 *A&A*, 625, A104
- Rigby, J. R., Bayliss, M., Sharon, K., Gladders, M., Chisholm, J., et al., 2018 *AJ*, 155, 104
- Rivera-Thorsen, T. E., Hayes, Matthew, Östlin, G., et al., 2015 *ApJ*, 805, 14
- Schaerer, D., 2003 *A&A*, 397, 527
- Schaerer, D., Fragos, T., & Izotov, Y. I., 2019 *A&A*, 622, 10
- Senchyna, P., Chisholm, J., Stark, D., Berg, D. A., James, B. L., et al. *in preparation*
- Shapley, A. E., Steidel, C. C., Pettini, M., & Adelberger, K. L., 2003 *ApJ*, 558, 65
- Stanway, E. R., Eldridge, J. J., & Becker, G. D., 2016 *MNRAS*, 456, 485
- Telford, O. G., Chisholm, J., McQuinn, K. B. W., & Berg, D. A., 2021 *ApJ*, 922, 191
- Thuan, T. X. & Izotov, Y. I., 2005 *ApJ*, 161, 240
- Veilleux, S., Cecil, G., & Bland-Hawthorn, J., 2005 *ARA&A*, 43, 769
- Verhamme, A., Orlitová, I., Schaerer, D., & Hayes, M., 2015 *A&A*, 578, A7
- Whitaker, K. E., Franx, M., Leja, J., et al., 2014 *ApJ*, 795, 104
- Wofford, A., Leitherer, C., & Salzer, J., 2013 *ApJ*, 765, 118